Available online at www.sciencedirect.com

ScienceDirect

Procedia Manufacturing 47 (2020) 1096–1100

Procedia MANUFACTURING

www.elsevier.com/locate/procedia

23rd International Conference on Material Forming (ESAFORM 2020)

Manufacturing of Isogrid Composite Structures by 3D Printing

Archimede Forcellese[a], Valerio di Pompeo[a], Michela Simoncini[a,b,*], Alessio Vita[a]

[a]*Università Politecnica delle Marche, Via Brecce Bianche 12, 60131 Ancona, Italy*
[b]*Università eCampus, Via Isimbardi 10, 22060 Novedrate (CO), Italy*

* Corresponding author. Tel.: +39 071 220 4443; fax: +39 071 220 4770. *E-mail address:* michela.simoncini@uniecampus.it

Abstract

In this research, isogrid panels in polyamide reinforced with short carbon fibers were manufactured by means of a 3D printing fused filament fabrication process. Before printing, the composite material was dried for 4 hours at 120°C in order to remove the humidity adsorbed by the polyamide. Then, during the printing process, the spool was kept at 70°C. The extrusion was performed at 240°C, with an infill density equal to 100%. The effect of geometric parameters, in terms of rib thickness and cell height, on the compressive strength and buckling behavior of the isogrid panels was investigated by means of compression tests carried out at room temperature on a servohydraulic testing machine. It was shown that the specific maximum compressive load at the onset of buckling increases with rib thickness. Furthermore, the isogrid panel characterized by the lowest cell height exhibits the highest specific maximum compressive load. Finally, the analysis of the isogrid panels after testing showed that failure is caused by global buckling failure mode; this suggests that the structure slenderness is higher than that of the ribs.

Keywords: Isogrid structures; Composite materials; 3D printing; Additive manufacturing; Fused filament fabrication; Buckling

1. Introduction

The use of composite materials in aerospace industry is a well-established procedure since they are characterized by high specific properties [1]. In some applications, for example propellant tanks for rockets, fuselage and boosters, the structures may be subjected to high axial compressive loads which could cause premature failure of the composite panels owing to buckling phenomena [2]. To avoid this, composite stiffening ribs can be used to provide more stiffness and strength. Typically, these stiffeners are manufactured in the form of equilateral triangles (isogrid structures) which are attached to the laminates [3].

Isogrid structures was investigated since '70s, when the National Aeronautics and Space Administration (NASA) published a report titled "Isogrid design handbook" [4]. In this publication, the manufacturing process of isogrid structures and their mechanical testing were studied. As these structures are subjected to axial compressive load, the failure might occur due to global buckling, if the slenderness of the panel is higher than the one of the ribs, or local buckling, if the slenderness of the ribs is higher than that of the panel [5]. Few researchers were addressed the optimization of these structures in order to maximize specific strength and stiffness. Wodesenbet et al. [6] investigated, through finite-elements analysis and experimentation, failure modes of a stiffened composite cylinders. They found that failure in global buckling mode resulted in higher specific load than the ones which fail in local buckling mode. In addition, they studied the effect of design parameters, such as skin thickness, skin winding angle, stiffener orientation angle and longitudinal modulus, on the specific resistance. Similarly, Jadhav et al. [7] optimized skin thickness, rib width and thickness and center-to-center distance between rib to maximize the specific energy absorption under transverse quasi-static and dynamic impact loading. They found a solution which maximize the specific strength using both FEM simulations and experiments. Zheng et al. [8] conducted the optimization of stiffened cylinder with a height

2351-9789 © 2020 The Authors. Published by Elsevier Ltd.

10.1016/j.promfg.2020.04.123

of 6 m and a diameter of 4 m through the use of finite element simulations. They suggested that the rib thickness should be larger than that rib width one due to the quadratic trend between critical force and thickness.

Isogrid structures were initially made of aluminum and were obtained by mechanical or chemical milling processes [4]. The improvement in the Automated Tape Laying (ATL) and Automated Fiber Placement (AFP) technologies has allowed the manufacturing of isogrid structures in carbon fiber reinforced plastics (CFRP) [9]. Kim [10] instead used a rubber tool to manufacture a isogrid structure. It was demonstrated, by axial compression tests, that this production method could represent an efficient system to achieve excellent stiffener consolidation and skin finish. Also manual processes, such as bag molding, were used to produce prototypes [11]. However, these methods require long manufacturing time and high costs, forcing researches and industry to adopt automated processes. Sorrentino et al. [12] used the filament winding technique to produce isogrid structures. Nevertheless, this technique is limited to axisymmetric components (cylinders) and the filament tension must be strictly controlled. All the automated manufacturing methods require significant investments which lead to high production costs, limiting the diffusion of these structures in the composite markets [13]. For this reason, researchers are focusing the attention on new manufacturing techniques such as additive manufacturing (AM) [14]. The 3D printing of composite materials is constantly under developing and under intense attention. However, there are some issues needed to be addressed including void formation, poor adhesion between fibers and matrix and increased curing time, especially when thermoset matrices are used [15]. The Fused Filament Fabrication (FFF) method, also known as Fused Deposition Modeling (FDM), is the preferred additive manufacturing technique to produce fiber reinforced materials [16]. Nevertheless, no research was found in literature concerning the 3D printing of composite isogrid structures. Only Li et al. [17] used 3D printing to study the resistance of novel T-rib hierarchical panels realized in PVC. It is evident a lack of knowledge in the field of composite isogrid structures obtained by means of additive manufacturing technologies.

In this framework, the present investigation aims at studying the feasibility of 3D printing production method for manufacturing of high performance isogrid panels in short fiber reinforced polyamide. Then, they were tested under compression load. An optimization of design parameters was performed in order to maximize the specific strength of the isogrid structures.

2. Design and fabrication

2.1. 3D printing

The Roboze One+400 professional FFF 3D printer, with a nozzle 0.6 mm in diameter, was used to produce the isogrid structures (Figure 1), in CarbonPA, a polyamide reinforced with 20% [wt] of short carbon fibers. According to the material datasheet, Carbon PA is able to match the mechanical strength of aluminum alloys, making it suitable for metal replacement applications in several sectors.

Fig. 1. The Roboze One+400 3D printer used for isogrid production.

Before printing, the composite material was dried for 4 hours at 120°C in order to remove the humidity adsorbed by the polyamide. Then, during the printing process, the spool was kept at 70°C. The extrusion was performed at 240°C, with an infill density equal to 100%. After 2 hours since printing, the isogrid panels were weighted.

2.2. Design of isogrid structures

The isogrid panels were obtained by crossing longitudinal ribs with ribs oriented at 60° and 120° with respect to the longitudinal ones (Figure 2); as a consequence, the single cell of isogrid structure was constituted by an equilateral triangle. Different values of the rib width (x) and cell height (t) were investigated, whilst, at this stage of the work, the rib thickness (z) was kept constant and equal to 4 mm. For each panel, the size of the sides parallel and perpendicular to the longitudinal ribs were kept constant and equal to 106 and 80 mm, respectively.

Table 1 summarizes the values of x, t and z, and the weight of each isogrid panel manufactured by means of the AM technology.

Table 1. Size and weight of the isogrid panels obtained by the fused filament fabrication process.

Isogrid Structure	Rib width, x [mm]	Rib thickness, z [mm]	Cell height, t [mm]	Weight [g]
4x8x18	4	8	18	55.6
4x8x24	4	8	24	56.1
4x9x18	4	9	18	58.9
4x9x24	4	9	24	60.1
4x10x18	4	10	18	64.3
4x10x24	4	10	24	65.5

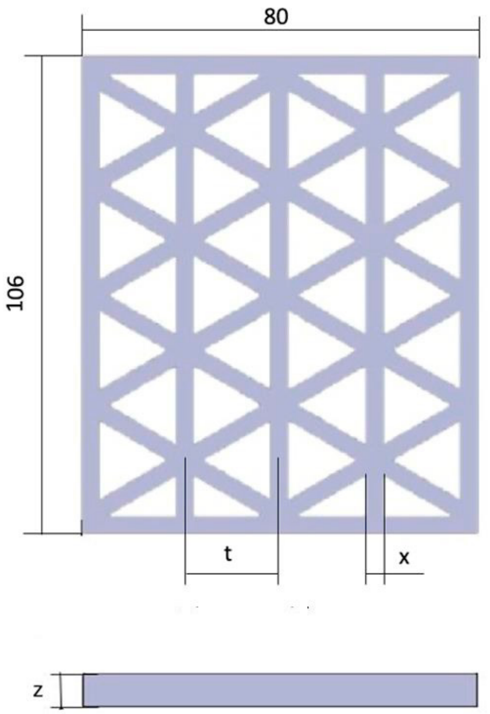

Fig. 2. Size and geometric variables of a typical isogrid panel with cell height equal to 24 mm.

Fig. 3. Compression test of an isogrid structure in short fiber reinforced polyamide.

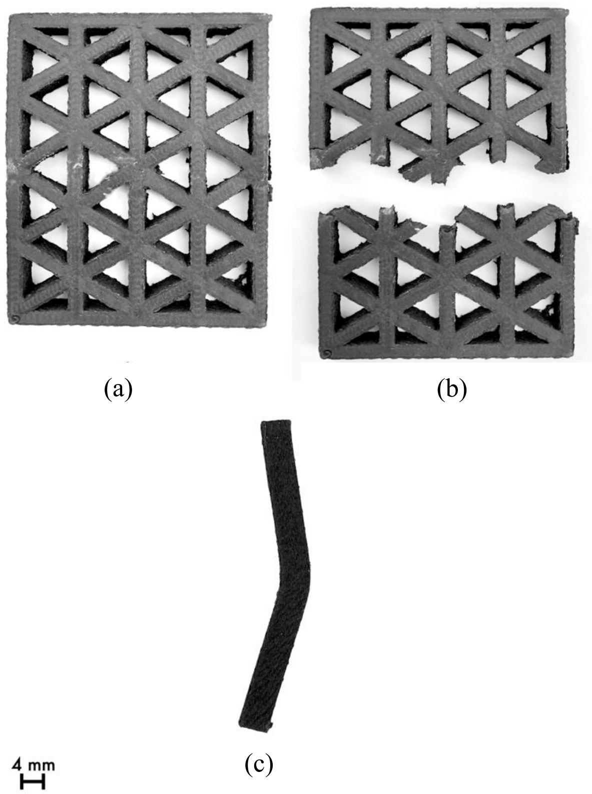

Fig. 4. (a) Front view of the undeformed isogrid structure, (b) front view of the isogrid structure after compression test; (c) side view of the isogrid structure after compression test (4x9x18).

2.3. Compression tests

In order to investigate the effect of geometric parameters on the buckling behavior of isogrid composites, room temperature compression tests were performed using the universal testing machine MTS 810, with a load capacity of 250 KN, equipped with two flat, smooth platens in tool steel (Figure 3). The head displacement rate was equal to 0.5 mm/min. During testing, the compressive load and platen displacement were acquired.

3. Results and discussion

Typical isogrid panels in short fiber reinforced polyamide, before and after compression test, are shown in Figure 4. By analyzing the isogrid panel after testing (Figure 4b), it can be observed that failure occurs owing to the global buckling failure mode characterized by instability that extends to the whole structure [18]. This behavior is more clearly shown by the side view of fractured isogrid (Figure 4c) and takes place in all the tested structures in the present work.

A magnification of typical fractured isogrid panel at a nodal intersection is shown in Figure 5. It clearly appears the occurrence of fracture due to the global buckling failure mode, indicating that the structure slenderness is higher than that of the ribs.

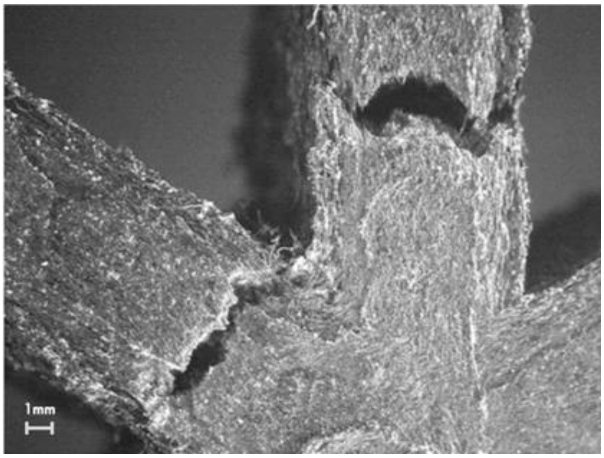

Fig. 5. Typical fractured isogrid panel at a nodal intersection (size: 4x10x18).

The results provided by compression tests of the isogrid panels were plotted as compressive load vs. platen displacement curves (Figure 6). It can be seen that, irrespective of the isogrid size, load increases with displacement until reaching a peak value corresponding to the onset of buckling failure mode; then, due to the occurrence of buckling, load decreases until fracture of the isogrid structure. For given rib thickness and rib width values, the peak value of compressive load vs. displacement curves decreases with increasing cell height. In addition, for given values of rib width and cell height, the peak value of compressive load vs. displacement curves increases with rib thickness.

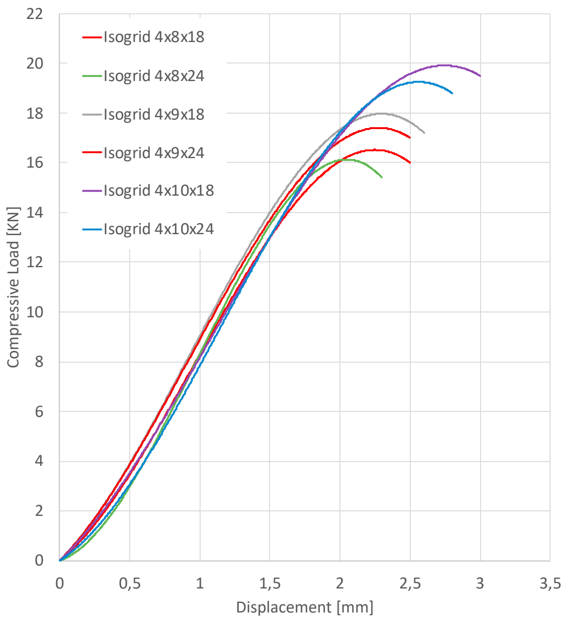

Fig. 6. Effect of the rib thickness and cell height on the compressive load vs. displacement curve of isogrid panels.

The maximum load applied during compression test of isogrid panels and the specific maximum load, obtained as the ratio between maximum load and panel weight, are summarized in Table 2.

The effect of the rib thickness and cell height on the specific maximum load is shown in Figure 7. Irrespective of the cell height, the specific maximum load rises with rib thickness. Such increase is more marked as the z value rises from 8 to 9 mm, whilst the growth rate tends to be lower as the thickness further increases from 9 to 10 mm. As far as the effect of the cell height is considered, it can be seen that the isogrid panels characterized by the lowest t value considered in the present work (18 mm) provide the highest specific maximum load value. The discrepancy in specific maximum load between the two cell heights investigated (18 and 24 mm) tends to rise as the rib thickness increases from 8 to 10 mm.

Table 2. Maximum load and specific maximum load of the isogrid structures in short fiber reinforced polyamide provided by compression tests.

Isogrid Structure	Maximum Load [KN]	Specific Maximum Load [KN/g]
4x8x18	16.5	0.3
4x8x24	16.1	0.285
4x9x18	17.9	0.31
4x9x24	17.4	0.29
4x10x18	19.9	0.312
4x10x24	19.1	0.293

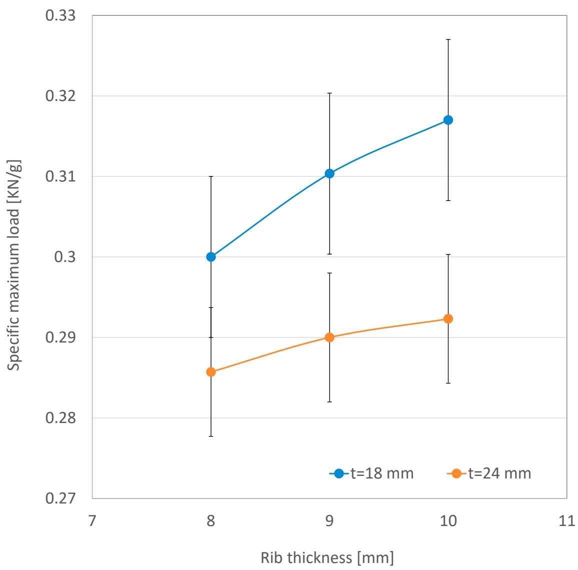

Fig. 7. Specific maximum load vs. rib thickness at different cell heights.

4. Conclusion

In the present work, isogrid panels in short fiber reinforced polyamide, with different values of rib thickness and cell height, were obtained by means of additive manufacturing. Then, they were subjected to compression test in order to investigate the effect of the geometric variables, in terms of rib thickness and cell height, on the compressive strength and buckling behavior of the isogrid structure.

The main results can be summarized as follows:

- the applied load rises with displacement during compression test of the isogrid panel until reaching a maximum value and then, due to the occurrence of buckling, decreases until fracture;
- the increase in cell height results in a decrease in both maximum load and specific maximum load whilst the increase in rib width leads to a rise in both peak load and specific maximum load;
- failure of the isogrid panel during compression test is due to the global buckling failure mode, indicating that the structure slenderness is higher than the one of the ribs.

Acknowledgments

This research was supported by POR FESR Abruzzo 2014/2020 – Linea di Azione I.1.1 e 1.1.4 – Avviso Pubblico per il "Sostegno a progetti di Ricerca Industriale, Sviluppo Sperimentale e Innovazione delle PMI nelle aree di specializzazione S3" (CUP: C37H18000070007).

References

[1] Holmes M. Carbon composites continue to find new markets. Reinf Plast 2017;61:36–40.
[2] Rahimi GH, Zandi M, Rasouli SF. Analysis of the effect of stiffener profile on buckling strength in composite isogrid stiffened shell under axial loading. Aerosp Sci Technol 2013;24:198–203.
[3] Totaro G. Local buckling modelling of isogrid and anisogrid lattice cylindrical shells with triangular cells. Compos Struct 2012;94:446–52.
[4] Meyer RR, Harwood OP, Harmon MB, Orlando JI. Isogrid design handbook 1973.
[5] Barbero E, Tomblin J. A phenomenological design equation for FRP columns with interaction between local and global buckling. Thin-Walled Struct 1994;18:117–31.
[6] Wodesenbet E, Kidane S, Pang S. Optimization for buckling loads of grid stiffened composite panels 2003;60:159–69.
[7] Jadhav P, Mantena PR. Parametric optimization of grid-stiffened composite panels for maximizing their performance under transverse loading 2007;77:353–63.
[8] Zheng Q, Jiang D, Huang C, Shang X, Ju S. Analysis of failure loads and optimal design of composite lattice cylinder under axial compression. Compos Struct 2015;131:885–94.
[9] Mack J, Mcgregor O, Mitschang P. Prepreg lay-up technology for manufacturing of lattice structure fuselage sections. 2014.
[10] Kim TD. Fabrication and testing of thin composite isogrid stiffened panel. Compos Struct 2000;49:21–5.
[11] Sorrentino L, Marchetti M, Bellini C, Delfini A, Albano M. Design and manufacturing of an isogrid structure in composite material : Numerical and experimental results. Compos Struct 2016;143:189–201.
[12] Sorrentino L, Marchetti M, Bellini C, Delfini A, Sette F Del. Manufacture of high performance isogrid structure by Robotic Filament Winding. Compos Struct 2017;164:43–50.
[13] Frketic J, Dickens T, Ramakrishnan S. Automated manufacturing and processing of fiber-reinforced polymer (FRP) composites: An additive review of contemporary and modern techniques for advanced materials manufacturing. Addit Manuf 2017;14:69–86.
[14] A. Forcellese, L. Greco, M. Pieralisi, M. Simoncini, G. Trevisan. Mechanical properties of carbon fiber reinforced plastic obtained by the automated deposition of an innovative towpreg. Accepted paper, Procedia CIRP 2020.
[15] Parandoush P, Lin D. A review on additive manufacturing of polymer-fiber composites. Compos Struct 2017;182:36–53.
[16] Wang X, Jiang M, Zhou Z, Gou J, Hui D. 3D printing of polymer matrix composites: A review and prospective. Compos Part B Eng 2017;110:442–58.
[17] Li M, Lai C, Zheng Q, Han B, Wu H, Fan H. Design and mechanical properties of hierarchical isogrid structures validated by 3D printing technique. Mater Des 2019;168:107664.
[18] Wang D, Abdalla MM. Global and local buckling analysis of grid-stiffened composite panels. Compos Struct 2015;119:767–76.